Electronic Supplementary Material (ESI) for Nanoscale.
This journal is © The Royal Society of Chemistry 2014

Electronic Supplementary Information

Characterization of TiO_2nanoparticles and TiO_2-filled rGO nanosacks

The nominal diameter of TiO_2 nanoparticles is <25 nm as provided in the vender specifications (Aldrich). To characterize the morphology and phase, TEM, dynamic light scattering (DLS) and X-ray diffraction (XRD) were used (Figure S1). The material is anatase TiO_2 with primary particle sizes from 20-30 nm. The encapsulation of TiO_2 with GO resulted in rGO nanosacks of 200 nm size filled with multiple TiO_2 nanoparticles (Figure S1B).

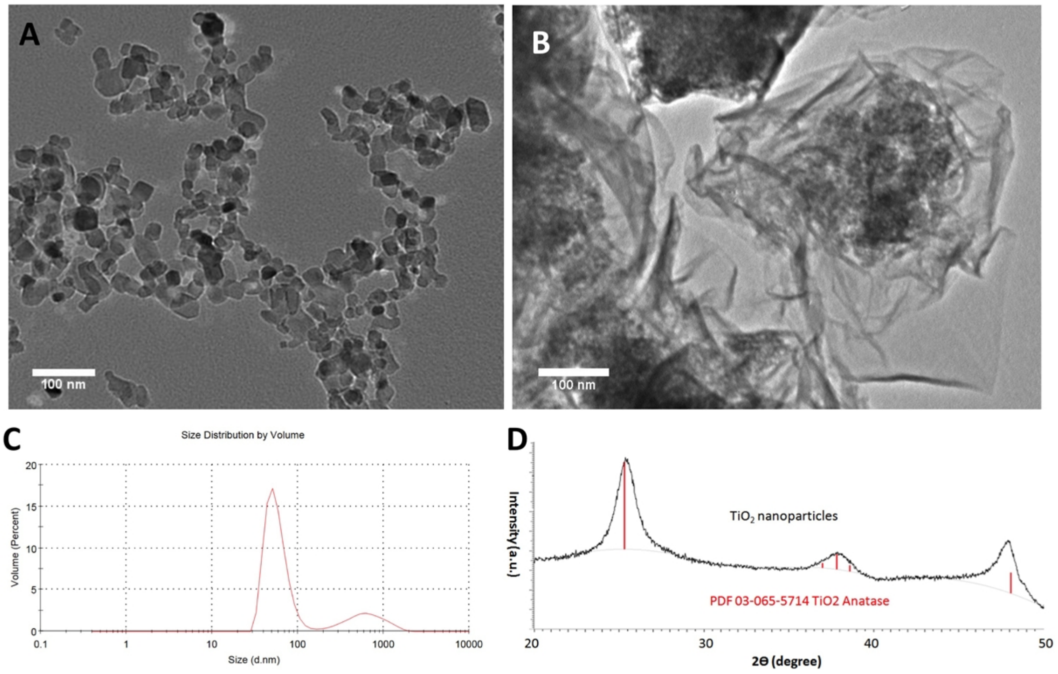

Figure S1. Morphology and phase of TiO_2nanoparticles and TiO_2-filled rGO nanosacks. A: the TiO_2 primary particles are 20~30 nm by TEM. B: The graphene nanosacks are 200-300 nm in diameter and contain multiple TiO_2 nanoparticles. C: the hydrodynamic diameters of the aggregates in aqueous media are around 57 nm with broad distribution by DLS. D: XRD pattern of TiO_2 nanoparticles (black curve) indicates they are mostly anatase nanoparticles according to the TiO_2 anatase reference pattern (red lines) of powder diffraction file (PDF).

Iron chelation by GO and its prevention

The introduction of iron salts can immediately induce aggregation and gelation of GO solution, indicating GO strongly binds to these multivalent ions. Such chelation can be prevented through adding excess level of much stronger chelator EDTA into iron solution before its introduction into GO solution. All the iron ions can be tightly trapped by EDTA and there is no free iron ion available for GO to capture, which was confirmed by measuring the Fe content left in solution after GO was removed. In that experiment, the solutions containing Fe-EDTA at the presence or absence of GO were incubated overnight and then centrifuged at 12,000 rpm for 20 min. The supernatants were collected and digested with concentrated nitric acid and concentrated by boiling. The resultant solutions were then diluted to get an estimated iron concentration of ~ 5 ppm in nitric acid (2%). The diluted solutions and standard solutions for calibration purpose were then fed into JY2000 Ultrace ICP Atomic Emission Spectrometer to measure the precise iron concentration. The calculated Fe content in the supernatants of initial solutions containing GO or not are 52.17±1.05 ppm and 52.94±1.58 ppm, respectively, indicating no measurable iron ion bonding to GO.

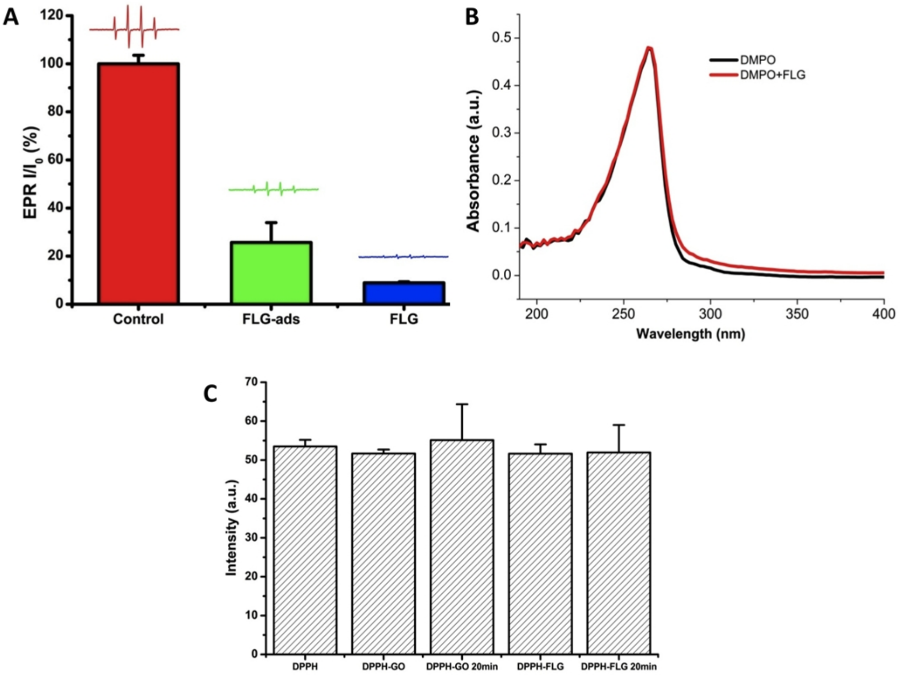

Figure S2. Study of potential interferences in the EPR experiments caused by the high hydrophobic surface area of FLG. A: FLG cause a large loss of the DMPO-OH EPR signal (blue bar) if it was present throughout the Fenton reaction. It can also cause significant loss of signal even though it was just introduced into the solution with existing DMPO-OH for a few seconds and quickly removed (green bar). All the signals have been normalized with the control solution (red bar). B: The absorbance of 100 mM DMPO solution around the characteristic absorption wavelength of 227 nm is similar to that pre-incubated with 100 ppm FLG, indicating negligible physical adsorption. C: DPPH adsorption by FLG does not cause distinct drop of EPR signal, implying no electromagnetic shielding. These data show that FLG reacts with both ·OH and the DMPO-OH adduct.

H_2O_2 decomposition by GO.

To test if GO can cause H_2O_2 decomposition a method based on cobalt oxidation was used to measure H_2O_2 concentrations before and after GO treatment. Briefly, cobalt (II) ions are oxidized by H_2O_2 to form a green complex with strong absorption around 310 nm. The H_2O_2 concentration in unknown samples can thus be determined through comparing its absorbance at 310 nm with that of calibration curve obtained from known samples.[1] After incubation with GO for 6 h in darkness, the concentration of H_2O_2 which was 10.00±0.28 mM before GO's introduction changed to 9.77±0.11mM, indicating a negligible decomposition of $H_2O_2$by GO during a reasonable period of time.

Potential artifacts in EPR study with FLG

It has been observed FLG shows high activity for ·OH scavenging in the study with EPR. To confirm the data are valid, we conducted further studies. The observed EPR signal (normalized peak intensity in the spectrum) of DMPO-OH adducts (Figure 2SA, blue bar) generated in the presence of 50 ppm FLG during Fenton reaction is less than 10% of the control solution (Figure 2SA, red bar). If the same amount of FLG is introduced after Fenton reaction and immediately removed, the signal (Figure 2SA, green bar) is less than 30% of the control, still a significant drop. This indicates FLG either (1) adsorbs DMPO/DMPO-OH adduct and shields the signal of adsorbed radical species or (2) scavenges the radical species (·OH and DMPO-OH adduct) at a fast rate. A DMPO adsorption study (Figure S2B) indicates the physically adsorbed DMPO by FLG is negligible compared with that in the bulk DMPO solution. So the drastic drop of EPR signal could only be due to the preferential adsorption of DMPO-OH adduct together with electromagnetic shielding if it is not due to fast radical scavenging. Then the potential screening effects by FLG/GO is thus studied with DPPH which is a much more stable radical species and can be quickly adsorbed by FLG (Figure S2C). GO does not affect the radical state of DPPH· regardless of their incubation time. It is interesting point that DPPH· maintains its detectable radical state even though it strongly binds FLG. The physical adsorption onto FLG is confirmed by the large drop of the DPPH· characteristic absorbance after FLG is introduced. The EPR signal of DPPH· does not change when FLG is introduce and the change is negligible even after 20 min incubation with FLG, featuring the absence of electromagnetic shielding effects. The results here thus rule out the first mechanism and confirm FLG as a strong scavenger of ·OH.

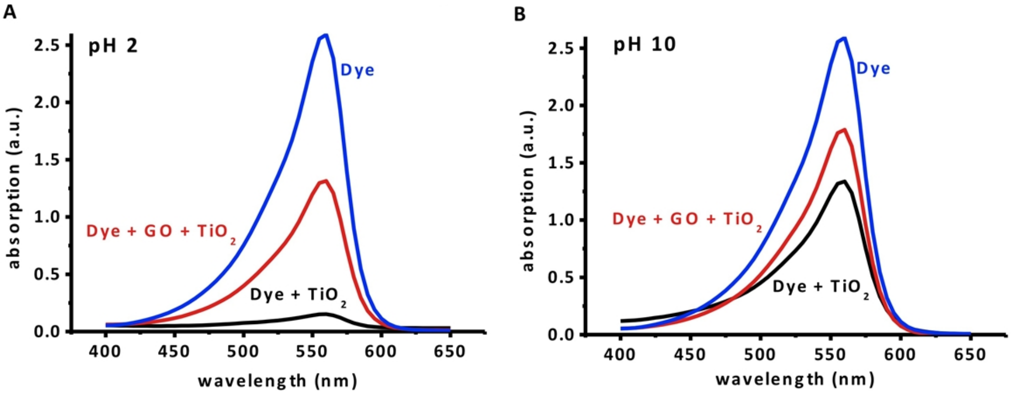

Figure S3. GO protects against photocatalytic damage by UV in the presence of TiO_2 in a pH independent manner. The protection effect at pH 2 (A) is similar to that at pH 10 (B) regardless the different photocatalytic decomposition rates.

TiO_2 photocatalytic protection at different pH values

The ability of GO to protect against photocatalytic damage by UV was studied at different pH values. Two solutions both containing 200 ppm TiO_2 and 200 ppm GO were adjusted to pH 2 and 10, respectively. The solutions were exposed to UV light for 10 h while agitated continuously on a rotor. The spectra were obtained after the UV irradiation, pH adjusted to 7.4 with PBS buffer and removal of GO and TiO_2. At pH 2 (Figure S3A) the TiO_2 is positively charged and GO is negatively charged and they form agglomerates in solution. At pH 10 (Figure S3B) TiO_2 and GO are both positively charged and a relatively more stable dispersion is obtained. Note the similar protection effects of GO at different pH. Electrostatic interaction brings GO in closer contact with TiO_2 but does not improve the radical scavenging effects. This suggests the protective effect is largely through radical quenching instead of TiO_2 surface passivation.

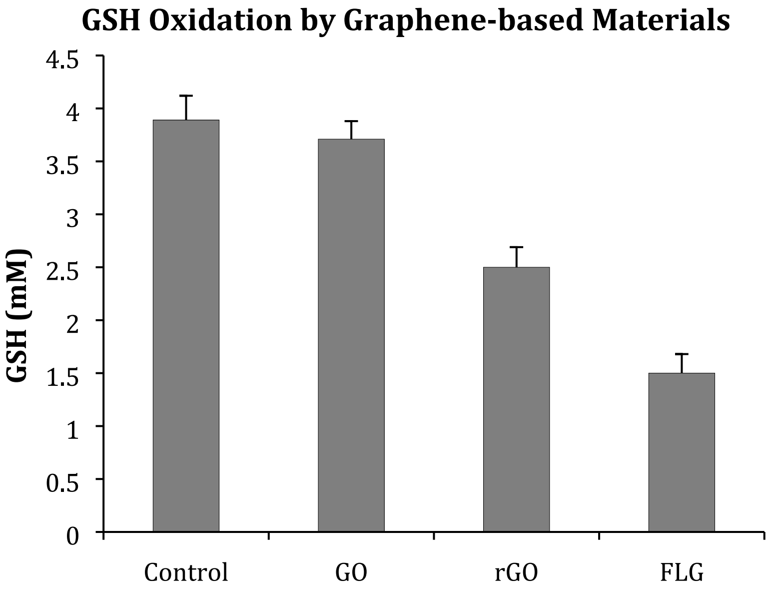

Figure S4. Intrinsic ROS generation by 40 ppm GO, rGO, FLG caused the oxidation of 4.0 mM GSH in pH 7.4 PBS.

Intrinsic ROS generation properties of graphene-based materials

The intrinsic ROS generation of GO, rGO and FLG was investigated with the GSH oxidation assay. 4 mM GSH was used as the indicator of materials' ROS generation in the pH 7.4 PBS aqueous solution. 12 hours after the introduction of 40 ppm graphene-based materials, the GSH concentrations were measured with the method as described in the main text. The GSH level in the solution containing FLG drops most significantly (Figure S4), indicating FLG produced the most ROS during the incubation. The overall order of oxidative properties from strong to weak is: FLG > rGO > GO. This indicates the actual antioxidant properties of FLG should be much stronger than the observed while the actual antioxidant properties of GO should be just a little bit stronger than the observed.

FTIR characterization on the graphene-based materials

The FTIR of three pristine graphene-based materials shows decreasing amount of hydroxyl groups and oxygen groups in the order: GO > rGO > FLG.

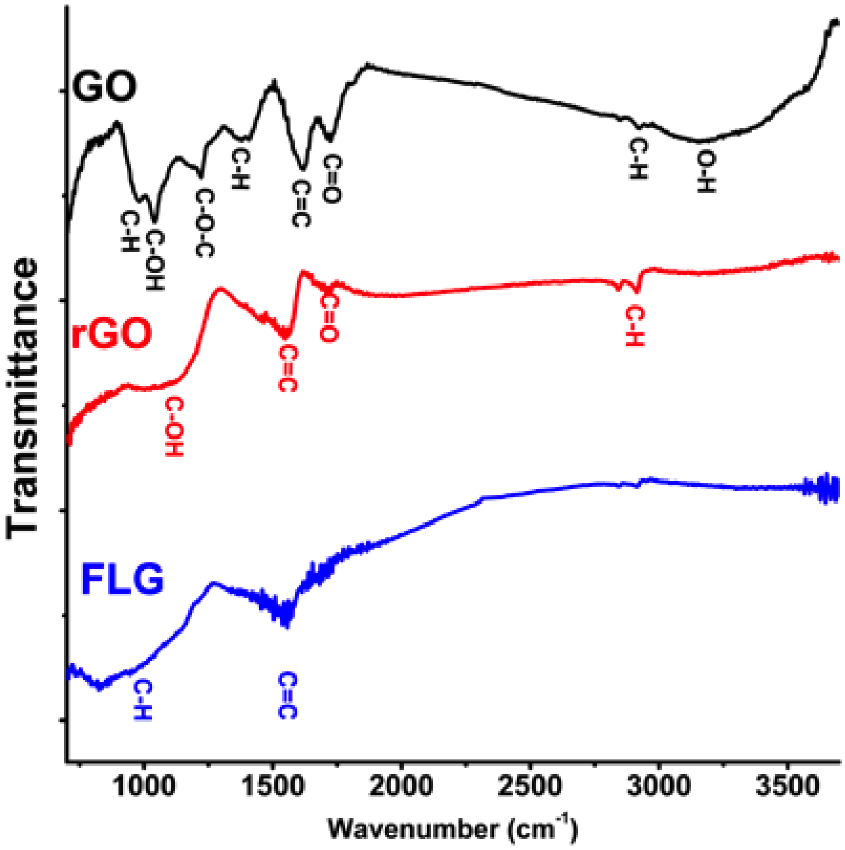

Figure S5. The FTIR of GO, rGO and FLG. The hydroxyl groups amount is decreasing in the order: GO > rGO > FLG.

Reference for Supplementary Data

1. D. Belhateche and J. M. Symons, *Journal American Water Works Association*, 1991, **83**, 70-73.